Received: 25 January 2019 | Accepted: 25 March 2019

DOI: 10.1111/gcb.14655

PRIMARY RESEARCH ARTICLE

Global Change Biology WILEY

# Testing early warning metrics for drought-induced tree physiological stress and mortality

William R. L. Anderegg[1] | Leander D. L. Anderegg[2,3] | Cho-ying Huang[4,5]

[1]School of Biological Sciences, University of Utah, Salt Lake City, Utah

[2]Department of Integrative Biology, UC Berkeley, Berkeley, California

[3]Department of Global Ecology, Carnegie Institution for Science, Stanford, California

[4]Department of Geography, National Taiwan University, Taipei, Taiwan

[5]Research Center for Future Earth, National Taiwan University, Taipei, Taiwan

**Correspondence**
William R. L. Anderegg, School of Biological Sciences, University of Utah, Salt Lake City, UT.
Email: anderegg@utah.edu

**Funding information**
U.S. Department of Agriculture, Grant/Award Number: 2018-67019-27850; National Science Foundation, Grant/Award Number: 1714972 , 1802880 and DBI-1711243; University of Utah; Ministry of Science and Technology, Grant/Award Number: 104-2119-M-002-034-; National Taiwan University, Grant/Award Number: NTU-107L9010; Ministry of Education

## Abstract

Climate change-driven drought stress has triggered numerous large-scale tree mortality events in recent decades. Advances in mechanistic understanding and prediction are greatly limited by an inability to detect in situ where trees are likely to die in order to take timely measurements and actions. Thus, algorithms of early warning and detection of drought-induced tree stress and mortality could have major scientific and societal benefits. Here, we leverage two consecutive droughts in the southwestern United States to develop and test a set of early warning metrics. Using Landsat satellite data, we constructed early warning metrics from the first drought event. We then tested these metrics' ability to predict spatial patterns in tree physiological stress and mortality from the second drought. To test the broader applicability of these metrics, we also examined a separate drought in the Amazon rainforest. The early warning metrics successfully explained subsequent tree mortality in the second drought in the southwestern US, as well as mortality in the independent drought in tropical forests. The metrics also strongly correlated with spatial patterns in tree hydraulic stress underlying mortality, which provides a strong link between tree physiological stress and remote sensing during the severe drought and indicates that the loss of hydraulic function during drought likely mediated subsequent mortality. Thus, early warning metrics provide a critical foundation for elucidating the physiological mechanisms underpinning tree mortality in mature forests and guiding management responses to these climate-induced disturbances.

**KEYWORDS**
climate change, drought, extreme events, plant hydraulics, remote sensing

## 1 | INTRODUCTION

Earth's forests provide trillions of dollars of benefits to society in ecosystem goods and services (Costanza et al., 1997) and take up nearly a quarter of human emissions of carbon each year, greatly slowing climate change (Bonan, 2008; Pan et al., 2011). Yet, human-caused climate change will profoundly alter the structure and function of forests through gradual changes in mean climate, disturbances, and increasing frequency of climate extremes such as heat and drought (Allen, Breshears, & McDowell, 2015; Bonan, 2008; IPCC, 2012). Climate extremes are expected to be damaging to ecosystems (Easterling et al., 2000) but the magnitude and spatiotemporal impacts of climate extremes on forests are particularly hard to predict because: (a) extremes are rare by definition; (b) the impacts often lag the inciting extreme by multiple years; and (c) experimental manipulation in the field is logistically difficult and thus inherently limited in scope, while greenhouse manipulation on small trees may not generalize to field settings. Thus, "natural experiments" of

  

assessments on mature forests during severe droughts are critical to develop a predictive understanding. However, such "natural experiments" are rare because such events are often missed and can only be studied retrospectively or opportunistically.

Severe drought and heat have triggered widespread forest die-off events in all forested biomes around the globe in recent decades (Allen et al., 2010, 2015; Hartmann et al., 2018). Tree mortality has manifold consequences for ecosystems, including decreases in biodiversity, increases in invasive species, and loss of ecosystem function (Anderegg, Kane, & Anderegg, 2013; Kane et al., 2011). Furthermore, tree mortality has the potential to influence land-atmosphere feedbacks through changes in forest biophysical and biogeochemical properties and even accelerate climate change if more carbon is emitted from dead trees than is absorbed by remaining living trees (Adams et al., 2010; Anderegg, Kane, et al., 2013). Despite mortality's critical impacts and potential carbon cycle feedbacks, our predictive understanding of drought-induced tree mortality remains quite limited (Adams et al., 2017; McDowell et al., 2011; Powell et al., 2013). Due in large part to the limitations described above, the vast majority of mortality physiology studies have been conducted in greenhouse settings, which limits their utility for improving global vegetation models (Adams et al., 2017).

Our ability to study and predict mortality is severely limited by not being able to determine which areas are likely to die from the inciting drought, and thus where measurements and/or management actions ought to be taken (Hartmann et al., 2018). This lack of an "early warning metrics" greatly constrains ecophysiological studies on mature forests and societal response to mortality (Hartmann et al., 2018). Ideally, such metrics would (a) use easily accessible and freely available satellite remote-sensing data, (b) be applicable in a broad array of forest systems, and (c) cover large spatial areas. Several early warning signals from remote-sensing techniques have been tried but efforts to date have some limitations because commonly utilized greenness indices, such as the Normalized Difference Vegetation Index (NDVI) (Rogers et al., 2018), may not have high accuracy in systems with high leaf area or where understory greenness responses obscure a mortality signal (Huete et al., 2002; Rogers et al., 2018), or because they are based on aircraft spectroscopic data that is costly and logistically not feasible for large geographic areas (Asner et al., 2016). Furthermore, the potential to link early warning metrics from remote sensing during the severe drought itself to tree physiological stress would provide an important advance for field ecophysiological studies to capture and quantify mortality mechanisms in vivo.

A "climate change-type" drought—a drought exacerbated by high temperatures—occurred in 2002 in the southwestern US and drove widespread mortality of trembling aspen (*Populus tremuloides*) in the region (Anderegg, Berry, Smith, et al., 2012; Huang & Anderegg, 2012; Worrall et al., 2008, 2010). However, like many drought-induced tree mortality events across the world (Anderegg, Berry, & Field, 2012; Trugman et al., 2018), we observed a lag between when drought struck and when mortality occurred (Figure 1). This lag was about 3–6 years (gray bars in Figure 1b)—new area affected by mortality peaked in 2007 and had largely tapered off by 2011. In previous work, we used freely available Landsat satellite data to show that we can map spatial patterns in the severity of drought-induced aspen mortality using the amount of "non-photosynthetically active vegetation (NPV)" cover (broadly defined as senescent leaves, bark, snags, and coarse woody debris) that can be directly viewed by a satellite optical sensor (Huang & Anderegg, 2012). Intriguingly, we found that NPV during the 2002 drought and the change in NPV between pre-drought and drought were indicative of areas that would experience high mortality between 2004 and 2010 (Figure 1) (Huang & Anderegg, 2014). Thus, we hypothesized these two metrics as potentially useful early warning metrics (Huang & Anderegg, 2014).

A second severe drought struck the region in 2012 (Figure 1a) and provided an excellent opportunity to rigorously field test the hypothesized early warning metrics. Guided by these early warning metrics from satellite data, we established a set of field plots during the severe 2012 drought, took a suite of physiological measurements, and followed these plots for subsequent mortality through 2017. We asked: (a) can the NPV-based early warning metrics during the 2012 drought explain subsequent mortality, (b) what are the potential canopy structural mechanisms underlying the early warning metrics, and (c) can the early warning metrics predict spatial patterns of tree water stress and physiological damage to guide ecophysiological field studies? As a preliminary investigation to test the generality of this approach in a very different system, we also did a simple analysis using the same metrics on the severe 2005 drought in the Amazon forest, which triggered substantial mortality (Brienen et al., 2015; Phillips et al., 2009, 2010).

## 2 | METHODS

### 2.1 | Overview

We used two consecutive droughts—2002 and 2012—in the same region to build and test early warning metrics for drought-induced tree mortality. The severe 2002 drought in the southwestern United States triggered a lagged episode of widespread aspen mortality, where mortality peaked at 4–5 years after the inciting drought (Worrall et al., 2008, 2010). Extensive research has shown that drought is the dominant cause of regional-scale aspen mortality in this area and time period (Anderegg, Berry, Smith, et al., 2012, Anderegg, Hicke, et al., 2015, Anderegg, Flint, et al., 2015; Worrall et al., 2008, 2010). Our focal study area was the San Juan National Forest (915 $km^2$; 37.5N, 108.3W, mean annual temperature = 3.9°C, mean annual precipitation = 699.7 mm) in western Colorado, USA (Huang & Anderegg, 2014), which experienced severe aspen mortality (Worrall et al., 2010).

We used previously hypothesized early warning metrics calculated from a satellite image taken during the severe 2012 drought to guide field plot selection and physiological measurements and then followed these satellite-selected plots and other existing field plots (see below) to observe lagged mortality 4–5 years later. This method provides a rigorous field test of early warning metrics because we did not know which, if any, of the plots would experience mortality 4–5 years later.

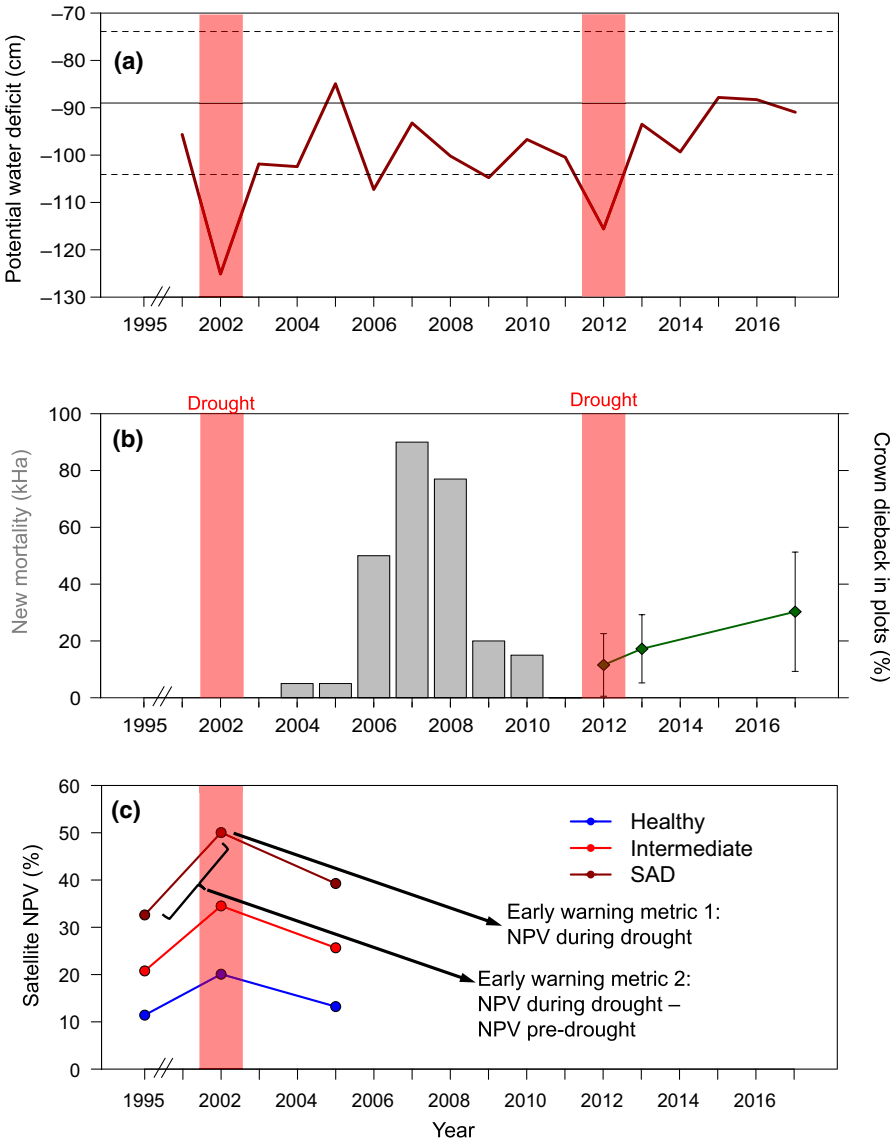


**FIGURE 1** (a) Potential water deficit (water year [October–September] precipitation—water year potential evapotranspiration) for the Upper San Juan (USGS HUC8 14080101) watershed from 2001 to 2017 from Abatzoglou, Dobrowski, Parks, & Hegewisch, 2018. Solid line is the mean from 1980 to 2000 and dashed lines are 1 standard deviation from the mean. (b) Lagged aspen mortality following two consecutive droughts (2002 and 2012; red shaded boxes) in the southwestern United States. Mortality data following the 2002 drought (gray bars, kHa of recent mortality per year) was taken from US Forest Service Aerial Detection Surveys over the state of Colorado and was redrawn from Worrall et al. (2010), calculated as the annual increase in the aspen damage area reported by Worrall et al. (2010). Green diamonds are average percent canopy dieback measured across all plots in the San Juan National Forest, Colorado and error bars are the standard deviation. (c) Blue, red, and dark red circles indicate the non-photosynthetically active vegetation (NPV) detected from Landsat for healthy, intermediate, and severe mortality/sudden aspen decline (SAD) affected plots, respectively, which were classified in 2011 in Huang and Anderegg (2014) based on field data in the same region (San Juan National Forest, CO). NPV-based early warning metrics illustrated via arrows

## 2.2 | Remote sensing of early warning metrics

Our previous studies conducted in the aspen forests of the San Juan National Forest found that the presence of a high amount of brown vegetation (NPV), indicating fewer leaves and more branches exposed to the sky, was able to accurately map spatial patterns in the severity of aspen mortality, whereas standard greenness indices could not (Huang & Anderegg, 2012). We also observed an increase in NPV during the drought (Figure 1c), which might reflect physiological response to drought through changes in leaf area or leaf shedding. This NPV increase was spatially correlated with subsequent (lagged) tree mortality patterns observed after the drought (2009–2011). Time-series analysis of NPV was undertaken in a previous study in these forests and found that NPV can robustly detect mortality at a regional scale (Huang & Anderegg, 2014).

In order to derive satellite NPV of 2011 and 2012 to test our early warning metrics, surface reflectance data of summer growing season Landsat Thematic Mapper (TM) (collected on July 1, 2011) and Enhanced TM plus (ETM+) (June 25, 2012) surface reflectance data for the San Juan National Forest were acquired from the LEDAPS (Landsat surface reflectance product processed using the on-demand processing Landsat Ecosystem Disturbance Adaptive Processing System) algorithm (Claverie, Vermote, Franch, Masek, 2015) via the Google Earth Engine servers via Python (https://earthengine.google.com/) (Figure S1). We controlled the dates of these two sets of imagery closely to make them comparable by sampling only in the ~2.5 month leaf area index (LAI) plateau in peak growing season of aspen forests and avoid natural seasonality induced differences in leaf development or senescence. Land surface endmember cover fractions photosynthetically active vegetation (PV), NPV, and bare soil (ranging from 0% to 100%) of each pixel were derived applying a Monte Carlo simulation-based spectral mixture analysis model (Bateson, Asner, & Wessman, 2000) using Interactive Data Language (IDL v. 8.2; Exelis Visual Information Solutions, Inc., CO, USA), which is ideal for the quantification of disturbed heterogeneous land surfaces (Huang et al., 2013). Specific settings for the

spectral mixture model for these aspen forests are described in previous publications (Huang & Anderegg, 2012, 2014). For the small amount of subsampled pixels corresponding to our field plots, we extended the unmixing repetition to 250K times to obtain a more stable outcome (Asner & Lobell, 2000).

## 2.3 | Plot locations and field data collection

We used the NPV calculated from the June 25, 2012 Landsat ETM+ image and the NPV12-NPV11 metric to identify 13 aspen plots that showed a wide range of early warning metric values (Figure S2). In particular, we conducted a stratified random sample within 1 km of an accessible road and selected ~54% of plots ($N$ = 7) that had NPV12-NVP11 >30% and 46% of plots ($N$ = 6) that had NPV12-NVP11 <30% in the same region. We also included two pre-existing plots, one with high NPV and one with low NPV, because we had strong baseline physiology and stand structure data pre-drought (2011; see Section 2.4 below). We ensured that none of these plots fell within the sections of missing data in Landsat 7 due to the Scan Line Corrector Failure, which is a well-known issue in Landsat 7 of data gaps due to a sensor failure (Chen, Zhu, Vogelmann, Gao, & Jin, 2011). This issue does not affect our study, however, as we used Landsat 7 only for calculating plot-level patterns (not region-wide patterns) and all of our plots did not fall in the image gaps. We surveyed those aspen plots from June 27 to July 3, 2012 and established 0.05 ha fixed radius (i.e., 8.8 m radius) circular plots, recording each plot's precise location with a Garmin Global Positioning System (spatial uncertainty <8 m). While these plots are relatively small compared to the pixel size, a smaller plot size was used both for feasibility constraints (high tree density precluded larger plots) and to reduce the potential for misregistration errors. Furthermore, plots were randomly located within larger, homogenous aspen forests and are thus likely to be representative and similar plot sizes have been used successfully to detect mortality with Landsat in these forests previously (Huang & Anderegg, 2012).

In each plot, we measured the diameter at breast height (DBH, cm, defined as stem diameter 1.37 m above the forest floor), status (living/dead), and percent canopy dieback (0%–100%) of all trees with a DBH greater than 5 cm. Percent canopy dieback in aspen is based on the number of recently dead branches and a visual assessment of the percentage of a roughly spherical healthy crown that is missing. All canopy dieback estimates were made by two independent observers and cross-checked for consistency, and we have used the percent canopy dieback metric extensively in remote sensing (Huang & Anderegg, 2012) and physiological (Anderegg, Berry, Smith, et al., 2012; Anderegg, Plavcová, et al., 2013) studies of aspen mortality previously. We also noted the presence of any secondary fungal or insect pests and pathogens in trees, which are thought to play a contributing but not a major causal role in aspen mortality in this region (Worrall et al., 2010). We resurveyed the plots in 2013 and 2017, measuring status and percent canopy dieback of each tree.

At these 13 satellite-selected and two pre-existing field plots, we took a suite of field measurements of physiology during the peak of the drought (June 27–July 5, 2012), which was just prior to the start of the monsoon rains that began around July 7, 2012 (see Anderegg, Anderegg, Berry, & Field, 2014 for detailed climate data during the drought). At these 15 plots, we measured the average leaf size and $\delta^{13}C$ of leaf sugars of mature, sun-exposed canopy leaves. We randomly selected three dominant canopy trees in each plot and between 12:00 and 14:00 hours collected two mid-to-upper canopy, sun-exposed branches with a 20 gauge shotgun, severing small branches with light bird-shot and ensuring that no leaves were damaged during collection. For leaf size, a random subsample of leaves from each tree was photographed immediately in the field (e.g., Figure 3a) and average leaf size was then calculated using ImageJ (https://imagej.nih.gov/ij/). At the pre-existing high and low NPV plots, we measured average leaf size using the exact same method (one plot in each group, three randomly selected trees per plot, ~30 leaves/plot) during August 15–16, 2011, and June 6–7, July 5–6, and August 15–16, 2012, which allows an assessment of the change between 2011 and 2012.

For $\delta^{13}C$ of leaf sugars, a separate random subset of leaves for each tree was immediately placed in sealed plastic bags and then in a dark cooler on ice. These leaves were kept in the dark and on ice until oven-dried at 65°C within 24 hr. Leaves were then ground finely using a Wiley Mill (30 mesh) and then ground to a powder using a ball mill. To extract the leaf sugars for isotopic measurements, we followed the ion chromatography protocol of Brugnoli, Hubick, Caemmerer, Wong, and Farquhar (1988) (Brugnoli et al., 1988; Richter et al., 2009). Briefly, 150 mg of ground leaf tissue was added to 150 mg of polyvinylpolypyrrolidone and 5 ml of DI water, vortexed for 5 s, and shaken at room temperature for 45 min. This sample was then centrifuged for 20 min at 17,000 *g*, and the supernatant recovered and used for chromatography. For sugar purification via chromatography, the supernatant was passed sequentially through an ion exchange resin (DOWEX 50Wx8-100, 50–100 mesh, SIGMA cat no. 217492) to eliminate amino acids and then an ion exchange resin (DOWEX 1X2, Cl-, 50–100 mesh, strongly basic, SIGMA cat no. 44290) to eliminate organic acids. Samples were then freeze-dried, foil-balled, and shipped to the UC Davis Stable Isotope Facility and measured via isotope ratio mass spectrometry (Thermoscientific) and $\delta^{13}C$ in parts per thousand notation (‰) was calculated as $\delta^{13}C = [(\delta^{13}C_{samp}/\delta^{12}C_{samp})]/[(\delta^{13}C_{ref}/\delta^{12}C_{ref}) - 1] \times 1{,}000$.

At a subset of seven plots (five satellite-selected and two pre-existing) selected to be in close geographic proximity but including four high NPV and three low NPV values, we took a further set of physiology and canopy measurements during the peak drought stress. We measured LAI using hemispherical photography at these seven plots during July 4–6, 2012. We took photographs prior to sunrise (05:00–06:00 hours) from the plot centers with a standardized orientation toward north. We then processed these photographs using Gap Light Analyzer (Frazer, Canham, & Lertzman, 1999) to calculate LAI with a standard angle of 75° because no plots were on steep (>10°) slopes. We measured predawn

and midday stem water potentials on three trees per plot and two sun-exposed branches per tree, collected as above and recut at least 20 cm and two distal nodes from the initial break point, using a Scholander-type pressure chamber (PMS Instruments, Corvalis OR, USA). Measurements were taken between 04:00 and 05:30 hours local time for predawn and 12:00–14:00 hours for midday and leaves were kept in the dark prior to measurement and measured within ~2 min after collection from the tree. Finally, we collected 2–3 branch segments from each of the three trees per plot to measure native and maximum stem hydraulic conductivity. Briefly, >10 cm segments were cut from branches (average branch diameter 0.5 cm) and kept dark and moist in a sealed plastic bag for transport to the laboratory. In the laboratory, branch segments were recut under water to avoid any cutting artifacts (Venturas, MacKinnon, Jacobsen, & Pratt, 2015) with a razor blade and then processed via the standard pressure-flow method (Sperry, Donnelly, & Tyree, 1988). Stems were then vacuum infiltrated overnight to remove any embolism and the process repeated to calculate maximum conductivity. Conductivity ($K_s$, g $m^{-2}$ $s^{-1}$ $MPa^{-1}$) was calculated standardized by branch basal area and stem length and the percent loss of conductivity (PLC, %) calculated as

$$PLC = 100 \times \left(K_{max} - K_{native}\right) / K_{max}$$

## 2.4 | Leveraging pre-existing field plots

In addition to the satellite-guided plots, we further leveraged existing aspen monitoring plots ($N$ = 15) in the San Juan National Forest, established between 2010 and 2014 with similar stand survey and dieback/mortality methods, from other research projects to track mortality between plot establishment and 2017. While these plots were selected for other reasons, primarily ecophysiological studies of aspen drought stress (Anderegg, Anderegg, Abatzoglou, Hausladen, & Berry, 2013; Anderegg et al., 2014), we extracted the 2011 and 2012 NPV values for the pixels in which they were located and they allowed us to bring additional sample sizes of aspen stands to bear on testing the early warning metrics for mortality ($N_{total}$ = 28 plots). These plot locations were selected randomly within larger aspen forests but typically constrained to be within 1 km of an accessible road for measurements.

## 2.5 | Analyses

We used ordinary least squares linear regression to test whether the early warning metrics could predict/explain eventual mortality or dieback. We analyzed two dependent variables—percent canopy dieback total (cumulative) in 2017 and the change in percent canopy dieback between 2012 (or plot establishment year) and 2017—and two independent variables—NPV during the 2012 drought ($NPV_{2012}$) and the difference in NPV from pre-drought to drought. We compared alternate models (single predictor variables, multiple variables, and interaction terms) using the Akaike information criterion. We had to drop two outlier plots—one where smoke from a fire contaminated the NPV calculation and one where a severe tent caterpillar outbreak confounded the drought signal with regard to mortality.

We compared the early warning metric $NPV_{2012}$ to stand structural (average leaf size and LAI) and physiological stress ($\delta^{13}C$ of leaf sugars, water potentials, $K_s$, and PLC) using univariate ordinary least squares linear regression. We checked the assumptions of linear regression using quantile–quantile and other diagnostic plots. All statistical analyses were conducted in the R software language, version 3.4 (R Core Team, 2012).

## 2.6 | Exploring the 2005 Amazon drought: Amazon field plot data

As a preliminary exploration of whether these early warning metrics might be useful across multiple biomes, we examined their applicability in the 2005 severe drought in the Amazon rainforest. We used the publicly available RAINFOR data for the Amazon from Brienen et al. (2015), available at forestplots.net. These are generally permanent sampling plots where the diameter and status of all trees within a 0.4–12 ha plot, depending on plot, was censused at irregular intervals. This data contains detailed aboveground biomass loss to mortality at each census from 1980 to 2011 with temporal normalization in Mg $ha^{-1}$ $year^{-1}$ and latitude/longitude coordinates for each plot at the tenth degree resolution (~10 km). We screened these plots for plots where an initial census was made in 2005 and a subsequent census was made in 2009 (to include previously documented lagged mortality post-drought but prior to a second drought in 2010), and excluded ones located in highly fragmented (likely human disturbed) forest landscapes. One plot recorded very high mortality rate in 2009 which was a normal year and 3 years after the 2005 drought, which was inconsistent with other plots. Therefore, we considered it as a potential "outlier" plot. We performed all analysis both with and without this plot. This led to a final sample size of 28–29 field plots (Table S1).

## 2.7 | Remote sensing of early warning metrics for the 2005 Amazon drought

The Amazonian validation data were widely distributed over a vast region. Therefore, the greenest period to determine the optimal time to assess pre-drought and drought PV and NPV may vary from plot to plot. To account for this, we acquired spatially corresponding high temporal resolution long-term (2001–2017) MODIS (the Moderate Resolution Imaging Spectroradiometer) EVI (the Enhanced Vegetation Index) to find the period (total 23 periods per year) with the maximum productivity. We found that the greenest periods of the studied region were within September 14 to November 1. We then acquired Landsat Thematic Mapper (TM) pixel values of the corresponding time period acquired in 2004 and 2005 from the Google Earth Engine servers via Python (https://earthengine.google.com/). The numbers of pixels selected were based upon the field plot sizes ranging from 0.4 to 12 ha.

Since no dimensions were described in the database, satellite pixels encompassing a circular plot shape were collected, which would also include most square plot designs. Fractional cover of the forested land surface's PV, NPV, and bare soil (ranging from 0% to 100%) of each pixel were calculated using the same spectral mixture analysis model applied on the aspen forests of San Juan National Forest but with tropical forest spectral endmembers; specific settings of the spectral mixture model for tropical forests can be found in Huang et al. (2013).

## 3 | RESULTS

Aspen canopy dieback in southwestern Colorado was initially low (11%) in these plots during the 2012 drought itself and rose slightly to 17% during 2013 (Figure 1b). However, by 2017, average plot canopy dieback was 32% with some plots reaching 50%–100% dieback (Figure 1b). These aspen canopy dieback and mortality rates are well above background rates of <10% average canopy dieback for healthy stands in this region (Huang & Anderegg, 2012) and <3% stem mortality rates during non-drought periods in the western United States in the US Forest Inventory and Analysis permanent monitoring plots (Anderegg, Hicke, et al., 2015; Anderegg, Flint, et al., 2015; Bell, Bradford, & Lauenroth, 2014). This timing of a 4–5 years lag in canopy dieback after the 2012 drought was consistent with the observed lag in dieback and mortality following the severe 2002 drought quantified in aerial surveys of aspen mortality in Colorado (Figure 1b). Collectively, the field plots covered a large range of dieback severity useful for testing the predictive accuracy of our early warning metric, including five plots that showed little canopy dieback indicative long-term, non-drought-related dieback rates (less than <10% by 2017).

The combination of early warning metrics for the 2012 drought which we had hypothesized based on our research on the 2002 drought—NPV during the drought and the change in NPV from pre-drought to drought—explained canopy dieback, particularly absolute canopy dieback levels in 2017, with high accuracy (Figure 2) (Dieback in 2017: $R^2 = 0.58$, $N = 26$, $df = 22$, $p < 0.0001$; change in dieback between 2012 and 2017: $R^2 = 0.23$, $N = 26$, $df = 22$, $p = 0.02$). The most parsimonious model (ΔAIC < −3 from all other models; Figure 2) showed that the canopy dieback in 2017 ($Dieback_{2017}$, %) was a function of NPV during the 2012 drought ($NPV_{2012}$) and the difference in NPV from pre-drought (2011) to drought (ΔNPV):

$$Dieback_{2017} = -0.93\,\Delta NPV + 0.92 NPV_{2012} + 2.78$$

with the intercorrelation of predictor variables of $r = 0.36$ and standard errors of the predictor variables as 0.21 and 0.17, respectively. The most parsimonious model for the change in canopy dieback between 2017 and 2012 had the same predictor variables:

$$\Delta Dieback = -0.33\,\Delta NPV + 0.43 NPV_{2012} + 1.61$$

with standard errors of the predictor variables as 0.18 and 0.15, respectively. The aim in including this latter dependent variable is to account for the variation in initial dieback conditions, as a few stands had higher levels of canopy dieback even in 2012, potentially from the previous 2002 drought.

Non-photosynthetically active vegetation is calculated using statistical methods from all Landsat reflective bands and is separated from "PV" and bare soil. Thus, NPV can be thought of as the amount of "exposed bark" in a 30 × 30 m pixel. Aspen plots with higher NPV generally showed more open and sparse canopies (Figure 3a). We found that NPV across plots was strongly associated with LAI during drought ($R^2 = 0.78$, $N = 7$, $df = 5$, $p = 0.008$, Figure 3d), but only weakly and insignificantly associated with average leaf size of sun-exposed leaves ($R^2 = 0.07$, $N = 15$, $df = 13$, $p = 0.4$, Figure 3c). For two plots where we had pre-drought data, the drought year was associated with both smaller average leaf size and a decrease in LAI (Figure 3b). These results suggest that the absolute NPV during drought is mediated by changes in canopy leaf area, but not necessarily average leaf size, which suggests that stressed forests may flush fewer leaves per branch or decrease the number of shade leaves.

Considering only the field plots selected entirely by the early warning metric from satellite data to capture a range of mortality risk, which were the plots where physiological measurements were made, NPV during the drought was strongly associated with several critical metrics of physiological stress that mediate mortality (Figure 4). NPV was associated with the $\delta^{13}C$ of leaf sugars ($R^2 = 0.39$, $N = 10$, $df = 8$, $p = 0.04$, Figure 4a) during the peak of the drought (early July 2012)

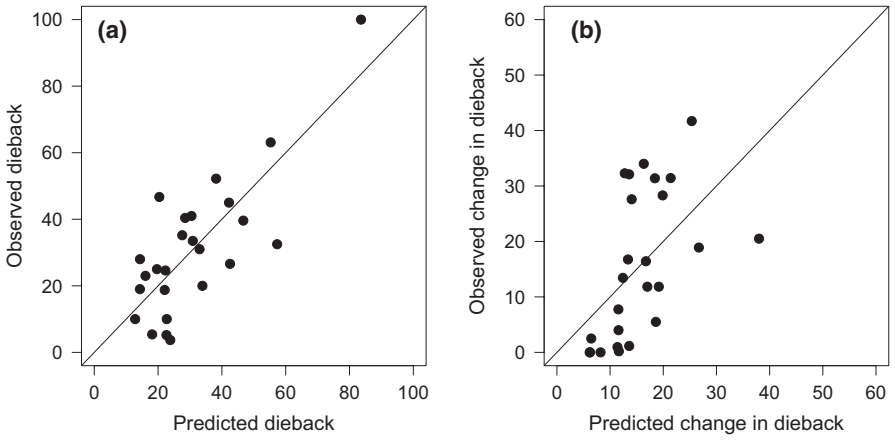


**FIGURE 2** (a) Regression-predicted percent total canopy dieback for aspen plots in 2017 and based on the satellite-derived early warning metrics during 2011 and 2012 compared to observed field-measured canopy dieback in 2017 ($R^2_{adj} = 0.58$, $p < 0.0001$). (b) Regression-predicted change in percent canopy dieback for aspen plots between 2012 and 2017 and based on the satellite-derived early warning metrics during 2011 and 2012 compared to observed field-measured change in dieback between 2012 and 2017 ($R^2_{adj} = 0.23$, $p = 0.02$). The black lines are the 1:1 lines

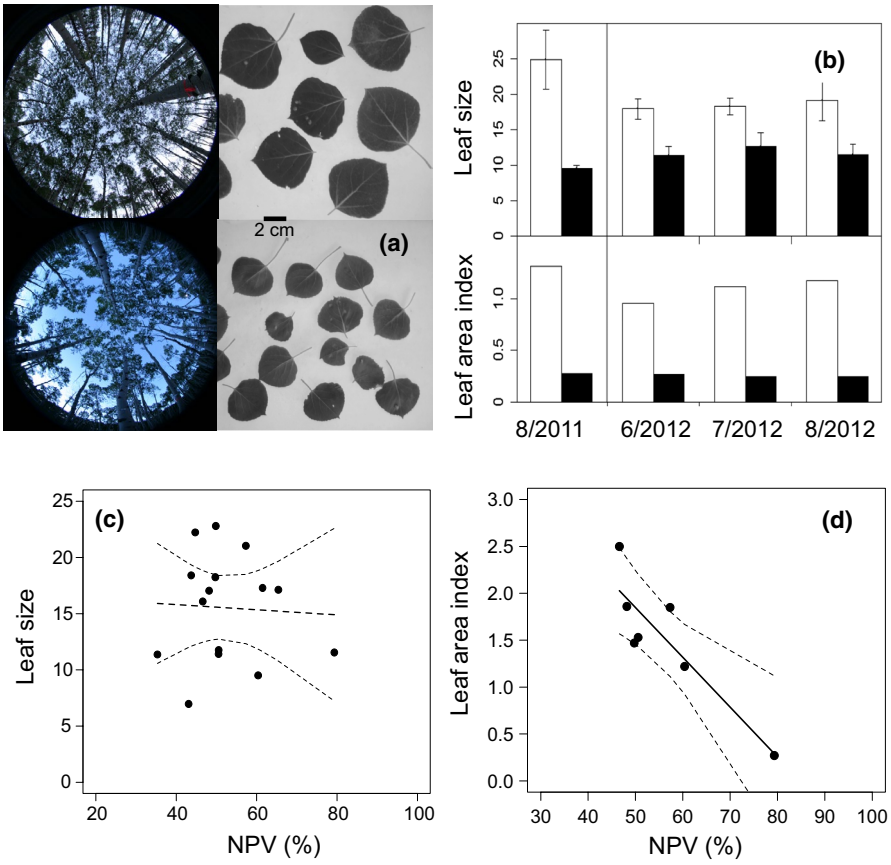


**FIGURE 3** Changes in canopy structure associated with satellite estimates of non-photosynthetically active vegetation (NPV). (a) Hemispherical photographs and average leaf size photos for a low NPV (top) and high NPV (bottom) aspen plot. The black line shows the scale bar. (b) Time-series of average leaf size ($N$ = ~25 leaves per stand per time window; $cm^2$) and leaf area index ($m^2/m^2$) of a low NPV (white bars) and high NPV (black bars) stand before and during the severe 2012 drought. (c and d) It shows the relationship between average leaf size ($cm^2$) and leaf area index, respectively, and NPV during the peak of the drought across 7–15 aspen plots. Lines are the ordinary least squares linear regressions with dashed lines showing the 95% confidence interval and solid lines are statistically significant; dashed regression lines are not statistically significant [Colour figure can be viewed at wileyonlinelibrary.com]

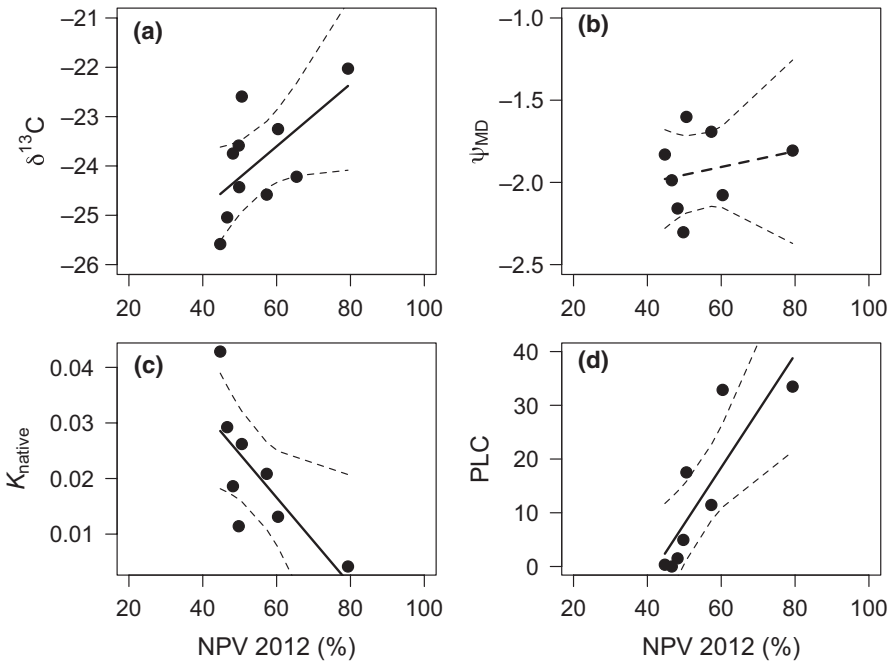


**FIGURE 4** Relationships between tree physiological variables and satellite estimates of non-photosynthetically active vegetation (NPV) during the peak 2012 drought. Physiological variables include (a) $\delta^{13}C$ of leaf sugars (‰; $R^2$ = 0.39), (b) midday stem water potential ($\psi$, MPa; $R^2$ = 0.09), (c) native stem hydraulic conductivity ($K_{native}$, g $m^{-2}$ $s^{-1}$ $MPa^{-1}$; $R^2$ = 0.54), and (d) percent loss of stem hydraulic conductivity (PLC, %; $R^2$ = 0.73). Lines are the ordinary least squares linear regressions with dashed lines showing the 95% confidence interval and solid lines are statistically significant; dashed regression lines are not statistically significant

with higher NPV stands showing more enriched values that are consistent with more frequent stomatal closure. The isotope ratio of $\delta^{13}C$ of leaf sugars likely captures the degree of recent stomatal closure (i.e., $C_i/C_a$) of the past 2–4 days in most species (Brugnoli et al., 1988). NPV was not associated with predawn ($p$ = 0.51) or midday ($p$ = 0.59) stem water potentials (Figure 4b). Nevertheless, NPV was strongly associated with both native stem hydraulic conductivity ($R^2$ = 0.54, $N$ = 10, $df$ = 8, $p$ = 0.03) and the percent loss of stem hydraulic conductivity ($R^2$ = 0.73, $N$ = 10, $df$ = 8, $p$ = 0.007) during the peak of the drought (Figure 4c,d).

As a preliminary analysis to test if the NPV metrics might predict subsequent mortality in other biomes, we calculated these same

metrics for 29 long-term forest plots that met our criteria in the Amazon following the severe 2005 drought. Both the difference between pre-drought and drought NPV ($R^2$ = 0.21, $N$ = 29, $df$ = 27, $p$ = 0.01) and the drought NPV ($R^2$ = 0.47, $N$ = 29, $df$ = 27, $p$ < 0.0001) metrics were significant predictors of aboveground biomass mortality by 2009. The most parsimonious model was a linear function of drought NPV that explained 47% of the variance in plot mortality (Figure S3) and 63% of the variance after removing one outlier plot where the mortality data may be incorrect (i.e., results are robust even with outlier included).

## 4 | DISCUSSION

Using data from two consecutive severe droughts, we have shown that publicly available satellite data can provide rigorous early warning metrics for drought-induced aspen mortality. In particular, the combination of the NPV during the drought and the change in NPV between pre-drought and drought were valuable early warning metrics of subsequent dieback and mortality. NDVI-based early warning metrics have been tested rigorously in North American boreal forests and found to capture both episodic pulses of mortality and more gradual "spiral of decline" in these forests (Rogers et al., 2018). This underscores that there may be multiple satellite-based optical remote sensing metrics that capture incipient mortality with different advantages and disadvantages. One advantage of an NPV-based approach is the ability to more clearly distinguish the signal of canopy dieback/mortality from understory vegetation, which is a limitation of NDVI-based approaches. Aspen forests are a useful study system to test early warning metrics for mortality because they have a multilayer canopy where our previous research found that the understory vegetation obscures mortality estimates based on greenness alone (Huang & Anderegg, 2012). And, indeed, NPV has been used to detect mortality and disturbance in a number of temperate and tropical forests (Chambers et al., 2007, 2013), although this has typically been larger scale mortality such as windthrow. Canopy leaf area adjustment is a widely observed phenomenon during drought (Barr et al., 2004, 2007; Sperry & Love, 2015) and our results suggest leaf area adjustment (a) can be observed via the amount of exposed non-photosynthetic tissue and (b) can be used to pick up stressed stands that might ultimately die.

Notably, satellite-derived NPV was strongly associated with multiple metrics of plant physiological stress during drought. This is particularly exciting because the majority of remote sensing based estimates of vegetation water stress have been conducted with airborne spectroscopic data (e.g., Asner et al., 2016) and stress detection with the freely available Landsat satellite data is potentially of broad interest. Loss of hydraulic conductivity through embolism and "hydraulic deterioration" has been shown to be a critical mechanism of drought-induced tree mortality after the 2002 and 2012 droughts in this species (Anderegg et al., 2014; Anderegg, Berry, Smith, et al., 2012; Anderegg, Plavcová, et al., 2013) and can predict spatial patterns in mortality following the 2002 drought (Anderegg, Hicke, et al., 2015; Anderegg, Flint, et al., 2015). As a caveat, we note that we do not have pre-drought physiological measurements on these plots and thus cannot rule out if these stressed plots had pre-existing/longer term hydraulic impairment due to previous droughts or poor site conditions. Indeed, it is unclear whether NPV is a good early warning metric because it identifies marginal sites that are most stressed at baseline and therefor most vulnerable to drought, or because it detects actual stress during drought. The fact that NPV goes up during drought (Figure 1c, Huang & Anderegg, 2012) indicates that NPV captures some element of drought stress. However, sites that subsequently die tend to have higher NPV at baseline (Figure 1), suggesting that our early warning model (including both $NPV_{2012}$ and $\Delta$NPV) may be driven by both site vulnerability and mid-drought stress. Disentangling these two signals is a fruitful avenue for future research.

The mechanisms of drought-induced tree mortality are an active research area (Adams et al., 2017; Hartmann et al., 2018) and while it was not our primary aim to directly quantify the mechanisms of mortality during the 2012 drought, the hydraulic status of aspen stands—whose locations were selected via the satellite early warning metric—during the drought was indeed predictive of eventual dieback/mortality in 2017 ($K_s$: $R^2$ = 0.53, $N$ = 8, $df$ = 6, $p$ = 0.04; PLC: $R^2$ = 0.79, $N$ = 8, $df$ = 6, $p$ = 0.003). We note, however, that the loss of hydraulic conductivity in our stands that subsequently died was much lower (e.g., 30%–40%) than currently hypothesized thresholds of ~60% (Adams et al., 2017). Thus, the intriguing finding that plant hydraulic status was identified from space suggests there is major promise in using satellites to guide mechanistic tree mortality studies. The lack of a relationship between NPV and stem water potentials is consistent with the lack of water potential differences between dying and healthy stands following the 2002 drought, where shifts in hydraulic vulnerability but similar water potentials led to loss in hydraulic function in dying stems (Anderegg et al., 2013). This lack of relationship between NPV and water potential may also be due to a suite of other things like soil texture, rooting distributions, and hydraulic traits that influence water potential that the satellite naturally cannot observe.

We believe these early warning metrics may be useful in a number of forest biomes, particularly broadleaf forest biomes with moderate to high LAI that form a large fraction of the terrestrial carbon sink. Indeed, our preliminary analysis in the Amazon rainforest during the severe 2005 drought supports this (Figure S3). There are some uncertainties and caveats that further studies are needed to explore. First, the spatial resolution of the publicly available geospatial coordinates adds uncertainty in colocating the field-measured dieback or mortality with remotely sensed NPV. Because we were careful to screen sites for continuous forest and these plots are predominantly in undisturbed mature forests, we believe this approach is still reasonable. Second, absolute NPV during the drought was the best predictor in the Amazon rather than both the difference between pre-drought

and drought NPV and the absolute NPV during the drought. This could either be because (a) region-specific (Amazon rainforest) endmembers are needed or (b) the LAI of these continuous forests is so high that NPV alone captures the majority of the important signal. Finally, as with all remote-sensing studies, the spatial scale mismatch between plot data and satellite pixels adds a source of uncertainty. While this Amazon analysis is exploratory and future work is needed to examine these metrics this region in more detail, it indicates that this early warning metric approach appears promising in a vastly different biome that is an important carbon sink and potentially threatened by rising climate-driven mortality (Brienen et al., 2015). A thorough understanding of the interactions between plant physiological mechanisms during mortality at the leaf and canopy scales and NPV is a critical avenue for future research, which could be assessed using canopy radiative transfer approaches (e.g., Féret, Gitelson, Noble, & Jacquemoud, 2017; Jacquemoud et al., 2009).

In conclusion, a set of early warning metrics for drought-induced tree mortality has extensive potential for a number of research fields and societal applications. A recent meta-analysis demonstrated that lags in mortality after drought are widely observed in many forest systems (Trugman et al., 2018). An early warning system of incipient tree mortality following drought thus presents an opportunity for managers to prepare treatments and trigger forest regeneration in managed forest settings (Cobb et al., 2017). With aspen, research has shown that treatment before canopy dieback reaches 30% typically yields robust forest regeneration while treatment after that threshold does not (Shepperd, Smith, & Pelz, 2015). For land management and mechanistic and modeling studies, there is a short "window of opportunity" between when drought strikes and all the trees have eventually died to improve our understanding of tree mortality and to improve forest resilience to climate extremes. Thus, there is major promise both for ecophysiologists, vegetation modelers, and land managers in developing and operationalizing an early warning system for drought-induced mortality.

## ACKNOWLEDGEMENTS

We thank K. Pham and M. Tassavoli for assistance with field and laboratory research. W.R.L.A. acknowledges funding from the David and Lucille Packard Foundation, the University of Utah Global Change and Sustainability Center, NSF grants 1714972 and 1802880, and the USDA National Institute of Food and Agriculture, Agricultural and Food Research Initiative Competitive Programme, Ecosystem Services and Agro-ecosystem Management, grant no. 2018-67019-27850. L.D.L.A. was supported by NSF grant no. DBI-1711243 and a NOAA Climate and Global Change postdoctoral fellowship. C.-y.H. was supported by the Ministry of Science and Technology (MOST) (104-2119-M-002-034-), National Taiwan University (NTU-107L9010) and Research Center for Future Earth, The Featured Areas Research Center Program, Higher Education Sprout Project, Ministry of Education (MOE) in Taiwan.

## ORCID

*William R. L. Anderegg* https://orcid.org/0000-0001-6551-3331
*Cho-ying Huang* https://orcid.org/0000-0002-9174-7542

## REFERENCES

Abatzoglou, J. T., Dobrowski, S. Z., Parks, S. A., & Hegewisch, K. C. (2018). TerraClimate, a high-resolution global dataset of monthly climate and climatic water balance from 1958–2015. *Scientific Data*, *5*, 170191. https://doi.org/10.1038/sdata.2017.191

Adams, H. D., Macalady, A. K., Breshears, D. D., Allen, C. D., Stephenson, N. L., Saleska, S. R., … McDowell, N. G. (2010). Climate-induced tree mortality: Earth system consequences. *Eos, Transactions American Geophysical Union*, *91*(17), 153–154. https://doi.org/10.1029/2010EO170003

Adams, H. D., Zeppel, M. J., Anderegg, W. R. L., Hartmann, H., Landhäusser, S. M., Tissue, D. T., … Allen, C. D. (2017). A multi-species synthesis of physiological mechanisms in drought-induced tree mortality. *Nature Ecology & Evolution*, *1*(9), 1285. https://doi.org/10.1038/s41559-017-0248-x

Allen, C. D., Macalady, A. K., Chenchouni, H., Bachelet, D., McDowell, N., Vennetier, M., … Cobb, N. (2010). A global overview of drought and heat-induced tree mortality reveals emerging climate change risks for forests. *Forest Ecology and Management*, *259*(4), 660–684. https://doi.org/10.1016/j.foreco.2009.09.001

Allen, C. D., Breshears, D. D., & McDowell, N. G. (2015). On underestimation of global vulnerability to tree mortality and forest die-off from hotter drought in the Anthropocene. *Ecosphere*, *6*(8), art129. https://doi.org/10.1890/ES15-00203.1

Anderegg, L. D. L., Anderegg, W. R. L., Abatzoglou, J., Hausladen, A. M., & Berry, J. A. (2013). Drought characteristics' role in widespread aspen forest mortality across Colorado, USA. *Global Change Biology*, *19*(5), 1526–1537. https://doi.org/10.1111/gcb.12146

Anderegg, W. R. L., Anderegg, L. D., Berry, J. A., & Field, C. B. (2014). Loss of whole-tree hydraulic conductance during severe drought and multi-year forest die-off. *Oecologia*, *175*, 11–23. https://doi.org/10.1007/s00442-013-2875-5

Anderegg, W. R. L., Berry, J. A., & Field, C. B. (2012). Linking definitions, mechanisms, and modeling of drought-induced tree death. *Trends in Plant Science*, *17*(12), 693–700. https://doi.org/10.1016/j.tplants.2012.09.006

Anderegg, W. R. L., Berry, J. A., Smith, D. D., Sperry, J. S., Anderegg, L. D. L., & Field, C. B. (2012). The roles of hydraulic and carbon stress in a widespread climate-induced forest die-off. *Proceedings of the National Academy of Sciences of the United States of America*, *109*(1), 233–237. https://doi.org/10.1073/pnas.1107891109

Anderegg, W. R. L., Flint, A., Huang, C.-Y., Flint, L., Berry, J., Davis, F., … Field, C. (2015). Tree mortality predicted from drought-induced vascular damage. *Nature Geoscience*, *8*, 367–371.

Anderegg, W. R. L, Hicke, J. A., Fisher, R. A., Allen, C. D., Aukema, J., Bentz, B., … Zeppel, M. (2015). Tree mortality from drought, insects, and their interactions in a changing climate. *New Phytologist*, *208*(3), 674–683. https://doi.org/10.1111/nph.13477

Anderegg, W. R. L., Kane, J. M., & Anderegg, L. D. L. (2013). Consequences of widespread tree mortality triggered by drought and temperature stress. *Nature Climate Change*, *3*(1), 30–36.

Anderegg, W. R. L., Plavcová, L., Anderegg, L. D. L., Hacke, U. G., Berry, J. A., & Field, C. B. (2013). Drought's legacy: Multiyear hydraulic deterioration underlies widespread aspen forest die-off and portends increased future risk. *Global Change Biology*, *19*(4), 1188–1196. https://doi.org/10.1111/gcb.12100

Asner, G. P., Brodrick, P. G., Anderson, C. B., Vaughn, N., Knapp, D. E., & Martin, R. E. (2016). Progressive forest canopy water loss during the 2012–2015 California drought. *Proceedings of the National Academy of Sciences of the United States of America*, *113*(2), E249–E255. https://doi.org/10.1073/pnas.1523397113

Asner, G. P., & Lobell, D. B. (2000). A biogeophysical approach for automated SWIR unmixing of soils and vegetation. *Remote Sensing of Environment*, *74*(1), 99–112.

Barr, A. G., Black, T. A., Hogg, E. H., Kljun, N., Morgenstern, K., & Nesic, Z. (2004). Inter-annual variability in the leaf area index of a boreal aspen-hazelnut forest in relation to net ecosystem production. *Agricultural and Forest Meteorology*, *126*(3–4), 237–255. https://doi.org/10.1016/j.agrformet.2004.06.011

Barr, Alan G., Black, T. A., Hogg, E. H., Griffis, T. J., Morgenstern, K., Kljun, N., … Nesic, Z. (2007). Climatic controls on the carbon and water balances of a boreal aspen forest, 1994–2003. *Global Change Biology*, *13*(3), 561–576. https://doi.org/10.1111/j.1365-2486.2006.01220.x

Bateson, C. A., Asner, G. P., & Wessman, C. A. (2000). Endmember bundles: A new approach to incorporating endmember variability into spectral mixture analysis. *IEEE Transactions on Geoscience and Remote Sensing*, *38*(2), 1083–1094.

Bell, D. M., Bradford, J. B., & Lauenroth, W. K. (2014). Forest stand structure, productivity, and age mediate climatic effects on aspen decline. *Ecology*, *95*(8), 2040–2046.

Bonan, G. B. (2008). Forests and climate change: Forcings, feedbacks, and the climate benefits of forests. *Science*, *320*(5882), 1444–1449. https://doi.org/10.1126/science.1155121

Brienen, R. J. W., Phillips, O. L., Feldpausch, T. R., Gloor, E., Baker, T. R., Lloyd, J., … Zagt, R. J. (2015). Long-term decline of the Amazon carbon sink. *Nature*, *519*(7543), 344–348.

Brugnoli, E., Hubick, K. T., von Caemmerer, S., Wong, S. C., & Farquhar, G. D. (1988). Correlation between the carbon isotope discrimination in leaf starch and sugars of C3 plants and the ratio of intercellular and atmospheric partial pressures of carbon dioxide. *Plant Physiology*, *88*(4), 1418–1424. https://doi.org/10.1104/pp.88.4.1418

Chambers, J. Q., Fisher, J. I., Zeng, H., Chapman, E. L., Baker, D. B., & Hurtt, G. C. (2007). Hurricane Katrina's carbon footprint on US Gulf Coast forests. *Science*, *318*(5853), 1107–1107.

Chambers, J. Q., Negron-Juarez, R. I., Marra, D. M., Di Vittorio, A., Tews, J., Roberts, D., … Higuchi, N. (2013). The steady-state mosaic of disturbance and succession across an old-growth Central Amazon forest landscape. *Proceedings of the National Academy of Sciences of the United States of America*, *110*(10), 3949–3954.

Chen, J., Zhu, X., Vogelmann, J. E., Gao, F., & Jin, S. (2011). A simple and effective method for filling gaps in Landsat ETM+ SLC-off images. *Remote Sensing of Environment*, *115*(4), 1053–1064.

Claverie, M., Vermote, E. F., Franch, B., & Masek, J. G. (2015). Evaluation of the Landsat-5 TM and Landsat-7 ETM+ surface reflectance products. *Remote Sensing of Environment*, *169*, 390–403.

Cobb, R. C., Ruthrof, K. X., Breshears, D. D., Lloret, F., Aakala, T., Adams, H. D., … Grünzweig, J. M. (2017). Ecosystem dynamics and management after forest die-off: a global synthesis with conceptual state-and-transition models. *Ecosphere*, *8*(12), e02034.

Costanza, R., d'Arge, R., De Groot, R., Farber, S., Grasso, M., Hannon, B., … Raskin, R. G. (1997). The value of the world's ecosystem services and natural capital. *Nature*, *387*(6630), 253.

Easterling, D. R., Meehl, G. A., Parmesan, C., Changnon, S. A., Karl, T. R., & Mearns, L. O. (2000). Climate extremes: Observations, modeling, and impacts. *Science*, *289*(5487), 2068–2074.

Féret, J. B., Gitelson, A. A., Noble, S. D., & Jacquemoud, S. (2017). PROSPECT-D: Towards modeling leaf optical properties through a complete lifecycle. *Remote Sensing of Environment*, *193*, 204–215.

Frazer, G. W., Canham, C. D., & Lertzman, K. P. (1999). Gap Light Analyzer (GLA), version 2.0. Imaging software to extract canopy structure and gap light transmission indices from true-colour fisheye photographs, users manual and program documentation. Simon Fraser University, Burnaby, British Columbia, and the Institute of Ecosystem Studies, Millbrook, New York, 36. Retrieved from http://citeseerx.ist.psu.edu/viewdoc/download?doi=10.1.1.458.1223&rep=rep1&type=pdf

Hartmann, H., Moura, C. F., Anderegg, W. R. L., Ruehr, N. K., Salmon, Y., Allen, C. D., … Galbraith, D. (2018). Research frontiers for improving our understanding of drought-induced tree and forest mortality. *New Phytologist*, *218*(1), 15–28.

Huang, C., & Anderegg, W. R. L. (2012). Large drought-induced aboveground live biomass losses in southern Rocky Mountain aspen forests. *Global Change Biology*, *18*(3), 1016–1027. https://doi.org/10.1111/j.1365-2486.2011.02592.x

Huang, C., & Anderegg, W. R. L. (2014). Vegetation, land surface brightness, and temperature dynamics after aspen forest die-off. *Journal of Geophysical Research: Biogeosciences*, *119*(7), 1297–1308.

Huang, C., Chai, C.-W., Chang, C., Huang, J.-C., Hu, K.-T., Lu, M.-L., & Chung, Y.-L. (2013). An integrated optical remote sensing system for environmental perturbation research. *IEEE Journal of Selected Topics in Applied Earth Observations and Remote Sensing*, *6*(6), 2434–2444.

Huete, A., Didan, K., Miura, T., Rodriguez, E. P., Gao, X., & Ferreira, L. G. (2002). Overview of the radiometric and biophysical performance of the MODIS vegetation indices. *Remote Sensing of Environment*, *83*(1–2), 195–213.

IPCC. (2012). *Managing the risks of extreme events and disasters to advance climate change adaptation. A special report of working groups I and II of the Intergovernmental Panel on Climate Change*. Cambridge, UK; New York, NY: Cambridge University Press.

Jacquemoud, S., Verhoef, W., Baret, F., Bacour, C., Zarco-Tejada, P. J., Asner, G. P., … Ustin, S. L. (2009). PROSPECT+ SAIL models: A review of use for vegetation characterization. *Remote Sensing of Environment*, *113*, S56–S66.

Kane, J. M., Meinhardt, K. A., Chang, T., Cardall, B. L., Michalet, R., & Whitham, T. G. (2011). Drought-induced mortality of a foundation species (*Juniperus monosperma*) promotes positive afterlife effects in understory vegetation. *Plant Ecology*, *212*(5), 733–741. https://doi.org/10.1007/s11258-010-9859-x

McDowell, N. G., Beerling, D. J., Breshears, D. D., Fisher, R. A., Raffa, K. F., & Stitt, M. (2011). The interdependence of mechanisms underlying climate-driven vegetation mortality. *Trends in Ecology & Evolution*, *26*(10), 523–532. https://doi.org/10.1016/j.tree.2011.06.003

Pan, Y., Birdsey, R. A., Fang, J., Houghton, R., Kauppi, P. E., Kurz, W. A., … Hayes, D. (2011). A large and persistent carbon sink in the world's forests. *Science*, *333*(6045), 988–993. https://doi.org/10.1126/science.1201609

Phillips, O. L., Aragao, L. E. O. C., Lewis, S. L., Fisher, J. B., Lloyd, J., Lopez-Gonzalez, G., … Torres-Lezama, A. (2009). Drought sensitivity of the Amazon rainforest. *Science*, *323*(5919), 1344–1347. https://doi.org/10.1126/science.1164033

Phillips, O. L., van der Heijden, G., Lewis, S. L., Lopez-Gonzalez, G., Aragao, L. E. O. C., Lloyd, J., … Vilanova, E. (2010). Drought-mortality relationships for tropical forests. *New Phytologist*, *187*(3), 631–646. https://doi.org/10.1111/j.1469-8137.2010.03359.x

Powell, T. L., Galbraith, D. R., Christoffersen, B. O., Harper, A., Imbuzeiro, H., Rowland, L., … Costa, M. H. (2013). Confronting model predictions of carbon fluxes with measurements of Amazon forests subjected to experimental drought. *New Phytologist*, *200*(2), 350–365.

Richter, A., Wanek, W., Werner, R. A., Ghashghaie, J., Jäggi, M., Gessler, A., … Gleixner, G. (2009). Preparation of starch and soluble sugars of plant material for the analysis of carbon isotope composition: A comparison of methods. *Rapid Communications in Mass Spectrometry*, *23*(16), 2476–2488. https://doi.org/10.1002/rcm.4088

Rogers, B. M., Solvik, K., Hogg, E. H., Ju, J., Masek, J. G., Michaelian, M., … Goetz, S. J. (2018). Detecting early warning signals of tree mortality

in boreal North America using multiscale satellite data. *Global Change Biology*, *24*(6), 2284–2304.

Shepperd, W. D., Smith, F. W., & Pelz, K. A. (2015). Group clearfell harvest can promote regeneration of aspen forests affected by sudden aspen decline in western Colorado. *Forest Science*, *61*(5), 932–937.

Sperry, J. S., Donnelly, J. R., & Tyree, M. T. (1988). A method for measuring hydraulic conductivity and embolism in xylem. *Plant, Cell & Environment*, *11*(1), 35–40. https://doi.org/10.1111/j.1365-3040.1988.tb01774.x

Sperry, J. S., & Love, D. M. (2015). What plant hydraulics can tell us about responses to climate-change droughts. *New Phytologist*, *207*(1), 14–27.

R Core Team. (2012). R: A language and environment for statistical computing. Retrieved from http://www.R-project.org/

Trugman, A. T., Detto, M., Bartlett, M. K., Medvigy, D., Anderegg, W. R. L., Schwalm, C., … Pacala, S. W. (2018). Tree carbon allocation explains forest drought-kill and recovery patterns. *Ecology Letters*, *21*, 1552–1560. https://doi.org/10.1111/ele.13136

Venturas, M. D., MacKinnon, E. D., Jacobsen, A. L., & Pratt, R. B. (2015). Excising stem samples underwater at native tension does not induce xylem cavitation. *Plant, Cell & Environment*, *38*(6), 1060–1068.

Worrall, J. J., Egeland, L., Eager, T., Mask, R. A., Johnson, E. W., Kemp, P. A., & Shepperd, W. D. (2008). Rapid mortality of *Populus tremuloides* in southwestern Colorado, USA. *Forest Ecology and Management*, *255*(3–4), 686–696. https://doi.org/10.1016/j.foreco.2007.09.071

Worrall, James J., Marchetti, S. B., Egeland, L., Mask, R. A., Eager, T., & Howell, B. (2010). Effects and etiology of sudden aspen decline in southwestern Colorado, USA. *Forest Ecology and Management*, *260*(5), 638–648. https://doi.org/10.1016/j.foreco.2010.05.020

## SUPPORTING INFORMATION

Additional supporting information may be found online in the Supporting Information section at the end of the article.

**How to cite this article:** Anderegg WRL, Anderegg LDL, Huang C-y. Testing early warning metrics for drought-induced tree physiological stress and mortality. *Glob Change Biol*. 2019;25:2459–2469. https://doi.org/10.1111/gcb.14655